Developments in Martensitic and Bainitic Steels: Role of The Shape Deformation

H. K. D. H. Bhadeshia
University of Cambridge
Materials Science and Metallurgy
Pembroke Street, Cambridge CB2 3QZ, U. K.
www.msm.cam.ac.uk/phase–trans

Abstract

Steels can be designed to exploit the coordinated motion of atoms during the bainite and martensite reactions. In this way it has been possible to make exceptionally strong and tough alloys in bulk form, and at an affordable price. Crystal sizes can be reduced to between 20–180 nm, by annealing heterogeneously deformed martensite, or by forming bainite under conditions where there is no atomic mobility.

Engineering failures are dominated by fatigue, the effects of which are exacerbated by welding and the associated residual stresses. Alloys can now be designed such that the deformation caused by transformation eliminates residual stresses, with extraordinary improvements in the fatigue life of constrained assemblies of metal. These important achievements are described here, within a framework which relates the atomic mechanism to the engineering scale.

INTRODUCTION

The matter of our everyday world is made up of atoms and it is the behaviour of collections of these entities which governs the properties of macroscopic samples. A good understanding of the various scales of matter is a fundamental goal of science, with the ultimate aim of creating predictive models. In this paper I hope to demonstrate, that in the context of steels, we have sufficient theory to create novel alloys without much experimentation or ad hoc parameters. The developments described deal with martensitic and bainitic steels, whose multi–scale structure depends on the trajectories of the atoms during the course of transformation. These trajectories are responsible for the macroscopic shape deformation, which in turn determines the microstructure. We begin therefore with a brief description of the characteristics and significance of this remarkable deformation which results from the synchronised motion of atoms.

SHAPE DEFORMATION

The conservative glide of a dislocation on a slip plane causes shear in a direction which lies in that plane. The material in the slip plane remains crystalline during the deformation, with no change in the relative positions of atoms on that plane, which is said to be *invariant* to the strain. Mechanical twinning is also a conservative mode of deformation and the plane on which the twinning shear occurs is similarly invariant.

If a material which has a Poisson's ratio equal to zero is uniaxially stressed below its elastic limit, then the plane that is normal to the stress axis is unaffected by the deformation since the only non-zero strain is that parallel to the stress axis (beryllium has a Poisson's ratio which is nearly zero).

All these strains belong to a class known as the *invariant–plane strains*, the operation of which leaves a plane undistorted and unrotated. Fig. 1a illustrates an invariant–plane strain (IPS) which is dilatational, and is of the type to be expected when a plate–shaped precipitate grows diffusionally. The change of shape is due to the volume change accompanying transformation. In Fig. 1b, the IPS corresponds to a simple shear at constant volume, as in slip or mechanical twinning.

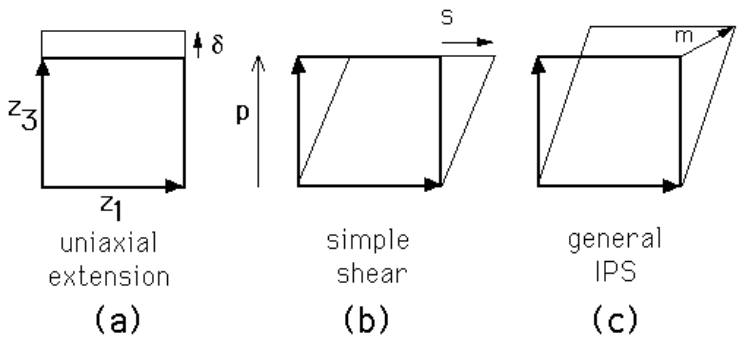

Fig. 1: Three kinds of invariant–plane strains. The squares indicate the shape before deformation. δ, s and m represent the magnitudes of the dilatational strain, shear strain and general displacement respectively. p is a unit vector, the shear strain s is parallel to z_1, whereas δ is parallel to z_3.

The most general IPS is a combination of dilatation and shear (Fig. 1c); if $\mathbf{d}$ is a unit vector in the direction of the displacements involved, then $m\mathbf{d}$ represents the displacement vector, where m is a scalar giving the magnitude of the displacements. $m\mathbf{d}$ may be factorised as $m\mathbf{d} = s\mathbf{z}_1 + \delta\mathbf{z}_3$, where s and δ are the shear and dilatational components, respectively, of the invariant–plane strain. Fig. 1c is representative of the shape deformation accompanying the formation of martensite or bainite, with $s \simeq 0.22$–0.26 and $\delta \simeq 0.02$–0.03. These deformations are much larger than elastic strains in a tensile test, which are of the order of 10^{-3}. s and δ therefore have profound effects on properties, as described below.

RESIDUAL STRESS

Manufacturing processes frequently introduce unwanted residual stress in mechanical parts [1], leading to a deterioration of fatigue–life. There are material factors which determine the type and magnitude of residual stress, for example, the heat capacity, thermal expansion coefficient, density and strength [2,3,4].

But in the context of steels, it has long been recognised that phase transformations can radically affect the development of residual stresses. Jones and Alberry [5] showed how the transformation temperature influences the evolution of stress as a constrained sample cools from the austenitic state (Fig. 2). The thermal expansion coefficient of austenite in lean steels is $e_\gamma \simeq 2.1 \times 10^{-6}\,\mathrm{K}^{-1}$ and that of ferrite is about $e_\alpha \simeq 1.3 \times 10^{-6}\,\mathrm{K}^{-1}$.

Thermal contraction of austenite therefore adds 400 MPa of tensile stress for each 100 K of cooling, given a Youngs modulus of 210 GPa. This is too large compared with the experimental data illustrated in Fig. 2, because at high temperatures the austenite relaxes by plastic

deformation to accommodate some of the thermal contraction. This is why the austenite part of the stress–temperature curve in Fig. 2 treks the yield strength as a function of temperature.

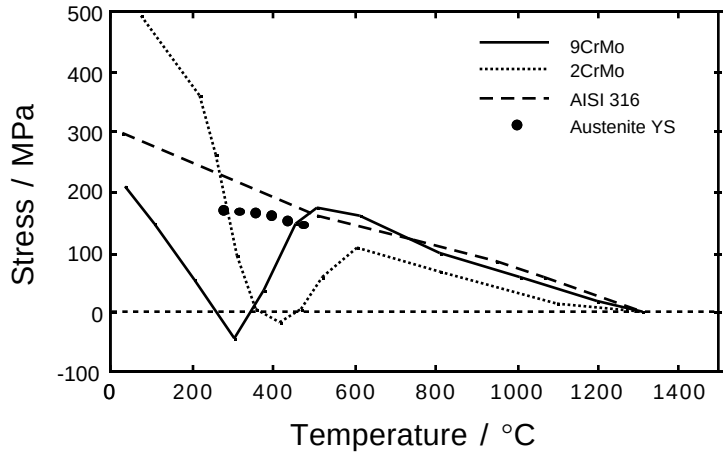

Fig. 2: Axial stress in uniaxially constrained samples during cooling of a martensitic (9Cr1Mo), bainitic ($2\frac{1}{2}$Cr1Mo) and austenitic steel (AISI 316). [5]. Also plotted is the yield strength of austenite [6].

The $2\frac{1}{2}$Cr1Mo sample begins to transform to bainite at about 600 °C. When this happens, the volume expansion due to the lower density of α–iron partly compensates for the contraction strain [7,8]. An important second effect is that those orientations of bainite form which best accommodate the macro–stress due to cooling. This bias in the microstructure prevents the shear strains of individual plates of bainite from being cancelled, as would happen in a random microstructure (where it is possible to find mutually accommodating plates) Fig. 3. The influence of a biassed microstructure can be much larger than the density change, because $s \gg \delta$ [9–20].

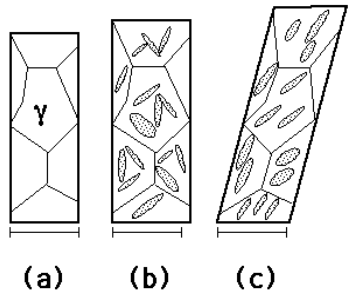

Fig. 3: Shape changes during unconstrained transformations. (a) Polycrystalline sample of austenite. (b) Displacive transformation into randomly oriented plates; the sample undergoes dilatational strain. (b) Transformed into an organised set of plates; the sample experiences both dilatation and shear.

It is significant that the Alberry and Jones' experiments show that the stress remaining at ambient temperature is smaller when the transformation temperature is reduced (*cf.* 9Cr1Mo and $2\frac{1}{2}$Cr1Mo steels). There are three reasons which explain this phenomenon:

(i) since $e_\gamma > e_\alpha$, the volume expansivity $3(e_\gamma - e_\alpha)\,\mathrm{K}^{-1}$ due to transformation is larger at lower temperatures, allowing a greater compensation of the accumulated thermal contraction strain.

(ii) If transformation becomes exhausted much before ambient temperature is reached, then it is the ferrite which contracts on cooling. Ferrite has a high yield strength (at low T) and hence there is a lesser compensation of contraction strain by plastic relaxation. This is why the stress rises sharply in the $2\frac{1}{2}$Cr1Mo steel after transformation is exhausted.

(iii) Transformation in constrained specimens, when it occurs at low temperatures, leads to a greater bias in the microstructure, making the shear strain s more prominent in mitigating thermal contraction. This is because there is a greater accumulation of stress before the low transformation–temperature is reached.

We now proceed to describe the exploitation of the phenomena described above.

FATIGUE

Many components are fatigue–limited. Cracks are initiated and grow slowly under the influence of an average stress which oscillates about some mean value, but which is below the yield strength as measured in a tensile test. The crack hopefully does not reach a critical value where fast–fracture occurs during the designated service life. The existence of residual stresses in the component effectively reduces the allowable applied stress.

It is often said that martensite "has a high dislocation–density". However, this is not a necessary feature of the transformation, since a glissile interface can move without creating defects. Dislocations are created if the IPS shape–change cannot be elastically accommodated. Whereas the shape–memory effect relies on the elastic accommodation of martensite, the circumstances are different in engineering steels where the martensite and bainite are plastically accommodated, resulting in the reported high dislocation–densities.

These dislocations can enhance the fatigue strength by increasing the resistance to plastic flow. This conclusion follows from the fact that prestraining a component (*i.e.* before fatigue loading) can increase the life [21], especially during low–strain fatigue [22]. The defects introduced by martensitic transformation provide an intrinsic "prestrain", and have been shown to improve the fatigue properties [23].

Whereas this effect of dislocation density is a natural consequence of the transformation, there has recently been a deliberate development by Ohta and co–workers [24–28], which follows from the Alberry and Jones work, and which is making significant waves in the engineering industries.

Fig. 4 illustrates distortion caused by welding, characterised in terms of the angle θ through which the unconstrained plates rotate as they cool following solidification. Table 1 shows θ as a function of the transformation temperature range, for two welding alloys deposited within a 60° V–joint. The distortion is clearly larger for the case where the transformation is exhausted at a higher temperature.

Ohta *et al.* designed a welding alloy with an exceptionally low transformation temperature

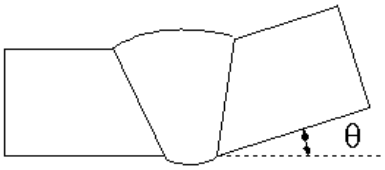

Fig. 4: Distortion caused by welding two plates which were originally flat. (Unpublished work, Bhadeshia and Svensson)

C / wt.%	Si	Mn	Ni	Mo	Cr	ΔT / °C	θ°
0.06	0.5	0.9	–	–	–	802–400	14.5
0.06	0.3	1.6	1.7	0.4	0.35	422–350	8

Table 1: The chemical compositions (wt.%), calculated transformation temperature range ΔT) and measured distortion θ for two manual metal arc, multipass weld deposits. (Unpublished work, Bhadeshia and Svensson).

(M_S), in which martensitic transformation in an unconstrained specimen starts at about 180 °C and is just completed at ambient temperature. By contrast, normal welding alloys have $M_S \simeq 500 - 400$ °C. As illustrated in Fig. 5a, the net strain (ϵ) on cooling between M_S and ambient temperature is a contraction in the case of the high–M_S "conventional" alloy, whereas there is a net expansion for the new welding alloy. This results in a large residual tensile stress for the high–M_S sample and a compressive one for the low–M_S alloy (Fig. 5b).

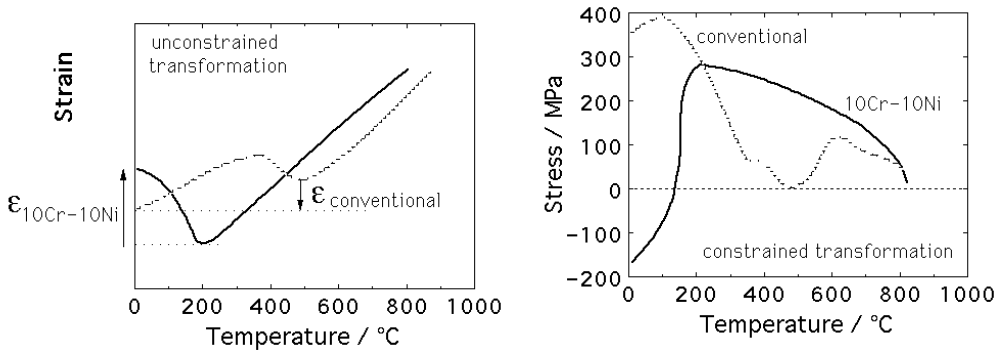

Fig. 5: (a) Transformation of weld metal during unconstrained cooling; (b) development of stress during constrained cooling. The chemical compositions of the alloys are given in Table 2. The low–M_S alloy is designated 10Cr10Ni in Table 2. After Ohta and coworkers.

When tests were done on welded sections, the structures joined using the low–M_S weld metal gave a much higher fatigue strength (Fig. 6). This improvement is attributed to the compressive residual stress which reduces the effective stress–range that the structure experiences

during fatigue testing. The results are spectacular for engineering; benefits of the order illustrated in Fig. 6 will lead to radical changes in design and lifing philosophies for structural components. The achievement is based entirely on the fact that the reduction of the transformation temperature allows the shape deformation to compensate for the accumulated thermal contraction strains. The work done in Japan has recently been confirmed by Ekerlid *et al.* [29].

Welding alloys used in civil constructions have to meet a range of requirements other than fatigue. Work is now needed to develop a system which gives a good portfolio of properties, such as strength, fatigue strength and toughness.

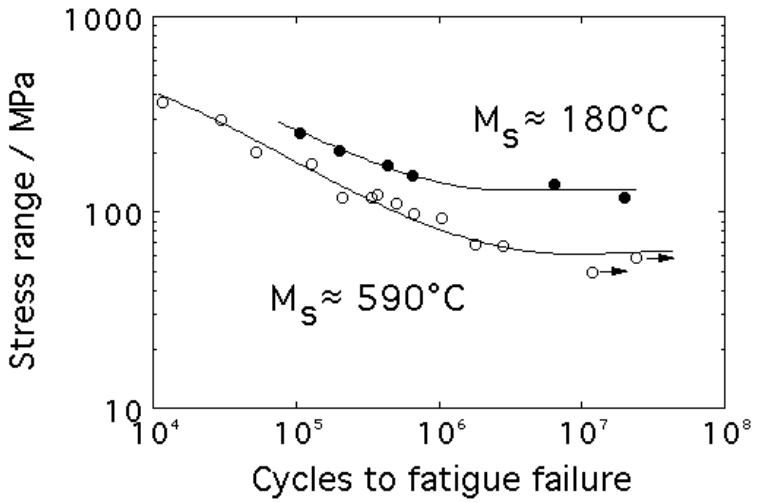

Fig. 6: Improvement in the fatigue performance of welded structure using a low transformation temperature welding alloy. After Ohta *et al.*.

Alloy	C / wt.%	Si	Mn	Ni	Mo	Cr	M_S / °C
Conventional	0.10	0.39	0.90	–	–	–	590
10Cr10Ni	0.025	0.32	0.70	10.0	0.13	10.0	180

Table 2: The chemical compositions (wt.%), and measured M_S temperature of conventional and novel welding alloys. After Ohta *et al.*

FINE GRAIN SIZE

A reduction of grain size frequently leads to an improvement in both the strength and toughness of a material. Sizes in the range 100–10 nm can be achieved using specialised laboratory techniques including rapid quenching and severe deformation ($\epsilon > 9$). However, these extreme processes are usually not practical on an industrial scale and more importantly, they are limited in the shapes that can be produced. The following sections show how fine grains can be achieved in bulk specimens by exploiting the atomic mechanism of martensitic and bainitic transformations.

Elastically Accommodated Plates

Displacive transformations in steels are associated with fine length scales because of the shape deformation. The strain energy density for martensite as a function of the transformation strains has been estimated using Eshelby's theory for a constrained transformation in which the phases remain coherent [30]. The elastic strain energy per unit volume (G_V^e) of a transformed region with the same shear modulus (μ) and Poisson's ratio (ν) as the isotropic constraining matrix is given by:

$$\begin{aligned} \frac{1-\nu}{\mu} G_V^e = & \overbrace{\frac{2}{9}(1+\nu)\Delta^2 + \frac{\pi t}{4l}\delta^2 + \frac{\pi t}{3l}(1+\nu)\Delta\delta}^{\text{contribution from volume change}} \\ & + \underbrace{\frac{\pi}{8}(2-\nu)\frac{t}{l}s^2}_{\text{contribution due to shear}} \\ \text{or} \qquad G_V^e \simeq & \frac{t}{l}\mu(s^2+\delta^2) \end{aligned} \tag{1}$$

where Δ is the uniform dilatation strain which is now known to be zero and the other strains s and δ are illustrated in Fig. 1. t and l are the thickness and diameter respectively of the oblate spheroid shape used to represent the martensite plate. For typical values of the parameters in equation 1, with $t/l = 0.05$, $G_V^e \simeq 600\ \mathrm{J\,mol^{-1}}$, which is large, and the reason why the plates tend to be thin.

Suppose it is assumed that a martensite plate can grow unhindered across an austenite grain of size $\overline{L}$, the mean lineal intercept. The maximum thickness of the plate is obtained by balancing the chemical free energy change accompanying transformation $\Delta G^{\gamma\alpha}$ against G_V^e, *i.e.*

$$t \simeq \frac{|\Delta G^{\gamma\alpha}| \times \overline{L}}{\mu(s^2+\delta^2)} \tag{2}$$

The plate thickness defines the mean free slip distance which is about $2t$ [31] and hence is the effective grain size. With these assumptions, the size of elastically accommodated martensite plates is related directly to the austenite grain size and the driving force for transformation. The mean size of the plates within a single austenite grain will be somewhat smaller than predicted because of the way in which the plates geometrically partition the parent phase. Notice how the shape deformation plays a vital role in determining the scale of the microstructure, with the shear strain dominating the equation.

Plastically Accommodated Plates

A displacive transformation involves the motion of a glissile interface. Just as in work–hardening, its motion can be halted by defects in the austenite. The defects can be created when the shape deformation due to martensite or bainite is accommodated by plastic relaxation of the surrounding austenite [32,33]. The growing plate then brings itself to a halt before it collides with the austenite grain surface. This is vividly illustrated by the sub–unit mechanism of bainite [34,35], in which an individual sheaf consists of a myriad of much smaller plates, each of which grows to a limited size which can be much smaller than that of the austenite grain.

Equation 2 indicates that during unhindered growth, thermoelastic equilibrium requires that the plates are coarser at low temperatures where $|\Delta G^{\gamma\alpha}|$ is largest. This contradicts observations because in practice the bainite is not in thermoelastic equilibrium; as stated earlier, there

is plastic relaxation in the adjacent austenite [33]. The resulting dislocation debris resists the advance of the bainite/austenite interface. Since austenite is weaker and dynamic recovery more likely at high temperatures, the plates in fact become thicker at elevated transformation temperatures. It is found that an increase in the strength of austenite by 100 MPa leads to approximately a 0.2 μm decrease in the thickness of bainite plates [36,37]; the intrinsic effects of $\Delta G^{\gamma\alpha}$ and temperature turn out to be much smaller in comparison.

The thickness must also be influenced by impingement between adjacent plates; as in all transformations, a large nucleation rate corresponds to a finer microstructure.

To summarise, transformation from strong austenite leads to fine plates when the shape deformation is plastically accommodated. The austenite can be made stronger by reducing the transformation temperature or by some other strengthening mechanism. Fig. 7a shows that by suppressing the bainite transformation to low temperatures, it is possible to obtain plates which are less than 40 nm in thickness, giving a strength in excess of 2500 MPa in a material which has considerable plasticity and toughness [38–41]. Fig. 7b illustrates the extent to which bainitic steels have progressed since the pioneering work of Irvine and Pickering in the 1950's. It has been possible to match and exceed the properties of the far more expensive marageing steels, by a combination of "grain refinement" as described above, and the elimination of carbide particles; the details are reviewed in [35]. Current efforts focus on extremely high–strength bainite (the point marked "4" on Fig. 7b).

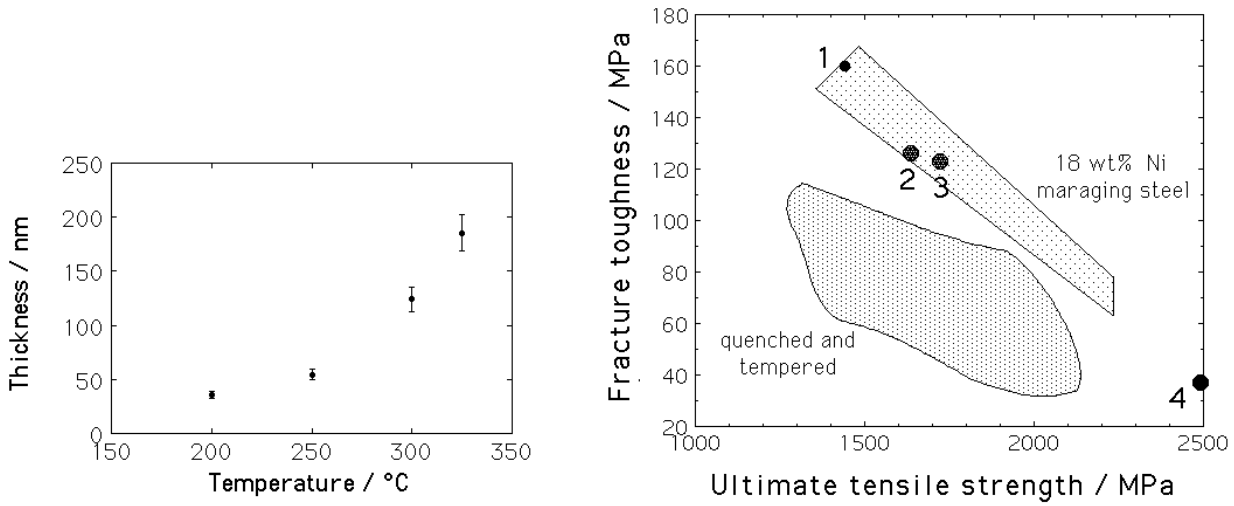

Fig. 8: (a) Stereologically corrected thickness of bainite plates as a function of the transformation temperature [41]. (b) The points marked 1, 2, 3 and 4 are all carbide–free bainitic steels.

Recrystallised Plates

When equiaxed grain structures are required, they can be generated by deformation followed by recrystallisation but in the context of current trends, this does not lead to a sufficiently fine grain structure. The extent of deformation needed also limits the form of the final product.

Tsuji and co–workers [42,43] have developed a process which avoids these difficulties by starting with a martensitic microstructure, which already has a high stored energy. To emphasise the latter point, calculated values of stored energies are listed in Table 3, where it can be seen that the magnitude is very large for martensite, even when compared against a mechanically–alloyed system. Martensite can therefore be recrystallised without any additional deformation. However, Tsuji *et al.* discovered that a small amount of plastic strain ($\simeq 50\%$) applied to a martensitic microstructure introduces three kinds of heterogeneities in the martensite, which have the effect of subdividing it. These are fine dislocation cells, irregularly bent laths and kinked laths and in each case the defect results in large local–misorientation, thereby providing ideal sites for the generation of new grains during annealing.

Defining grain size in terms of regions with a critical level of misorientation, the original martensite was judged to have a grain size of 3.2 μm. Its subdivision by heterogeneous deformation, led by the same definition, to an equiaxed grain size of about 180 nm after annealing, a reduction in scale by a remarkable factor of 18.

Phase Mixture in Fe–0.2C–1.5Mn wt.% at 300 K	Stored Energy / J mol^{-1}
1. Ferrite, graphite & cementite	0
2. Ferrite & cementite	70
3. Paraequilibrium ferrite & paraequilibrium cementite	385
4. Bainite and paraequilibrium cementite	785
5. Martensite	1214
6. Mechanically alloyed ODS metal	55

Table 3: The stored energy as a function of microstructure, relative to the equilibrium state defined as a mixture of ferrite, cementite and graphite [44]. The phases in cases 1 and 2 involve a partitioning of all elements so as to minimise free energy. In cases 3–5 the iron and substitutional solutes are configurationally frozen (for martensite even the interstitial elements are frozen). Case 6 refers to an iron–base mechanically alloyed oxide–dispersion strengthened (ODS) sample which has the highest reported stored energy prior to recrystallisation [45].

SUMMARY

The simple recognition that the invariant–plane strain shape deformation observed during the course of martensitic and bainitic transformations results in large elastic and plastic strains, and the fact that these strains must be accommodated in the surrounding austenite, has led to the design of some extraordinary steels. The advances are remarkable given the current emphasis on everything "nano", for here are mechanisms which lead to nano–scale structures in bulk samples at reasonable costs. It is no wonder that most of the developments discussed here are now available commercially.

ACKNOWLEDGMENTS

The author is grateful for financial support from the Engineering and Physical Sciences Research Council, U. K.

REFERENCES

1. J. Lu: *Handbook of Residual Stress and Deformation of Steel,* eds G. Totten, M. Howes and T. Inoue, ASM International, Materials Park, Ohio (2002) 11-26.
2. H. K. D. H. Bhadeshia: *Handbook of Residual Stress and Deformation of Steel,* eds G. Totten, M. Howes and T. Inoue, ASM International, Materials Park, Ohio (2002) 1-10.
3. P. J. Withers and H. K. D. H. Bhadeshia: *Materials Science and Technology* **17** (2001) 355–365.
4. P. J. Withers and H. K. D. H. Bhadeshia: *Materials Science and Technology* **17** (2001) 366–375.
5. W.K.C. Jones and P.J. Alberry: *Metals Technology* **11** (1977) 557–566.
6. P.H. Shipway and H.K.D.H. Bhadeshia: *Materials Science and Engineering A* **A201** (1995) 143–149.
7. G. W. Greenwood and R. H. Johnson: *Proceedings of the Royal Society* **238** (1965) 403–422.
8. R. H. Johnson and G. W. Greenwood: *Nature* **195** (1962) 138–139.
9. C. L. Magee: *Ph. D. Thesis* Carnegie Mellon University, Pittsburgh, USA, (1966.)
10. C. L. Magee and H. W. Paxton: *Trans. Met. Soc. AIME* **242** (1968) 1741–1749.
11. F. D. Fischer: *Acta Metall. Mater.* **38** (1990) 1535–1546.
12. J. B. Leblond, G. Mottet and J. C. Devaux: *J. Mech. Phys. Solids* **34** (1986) 395–409; 411–432.
13. J. B. Leblond, J. Devaux and J. C. Devaux: *International Journal of Plasticity* **5** (1989) 551–572.
14. J. B. Leblond: *International Journal of Plasticity* **5** (1989) 573–591.
15. J. B. Leblond and J. Devaux: *Residual Stresses,* Elseviers, New–York (1989) 1–6.
16. J. B. Leblond: *Internal Report CSS/L/NT/90/4022,* FRAMASOFT, Paris (1990) 1–12.
17. G. B. Olson: *Deformation, Processing and Structure,* American Society of Metals, Metals Park, Ohio, U.S.A., (1982) 391–424.
18. H. K. D. H. Bhadeshia, S. A. David, J. M. Vitek and R. W. Reed: *Materials Science and Technology* **7** (1991) 686–698.
19. A. Matsuzaki, H. K. D. H. Bhadeshia and H. Harada: *Proceedings of ICOMAT '92,* Monterey, California, USA, eds. C. M. Wayman and J. F. Perkins, published by the Monterey Institute for Advanced Studies (1992) 749–754.
20. A. Matsuzaki, H. K. D. H. Bhadeshia and H. Harada: *Acta Metallurgica et Materialia* **42** (1994) 1081–1090.
21. D. Cratchley and J. Smith: *J. Iron Steel Institute* **203** (1965) 461–467.
22. C. Laird: *Metallurgical Transactions A* **8A** (1977) 851–860.
23. H. R. Sander and M. Hempel: *Arch. Eisenhuettenw.* **23** (1952) 299-320.
24. C. Shiga: *Science and Technology of Welding and Joining* **5** (2000) 356–364.
25. J. Yamamoto, Y. Muramatsu, S. Zenitani, N. Hayakawa and K. Hiraoka: *6th Int. Conf. on Trends in Welding Research,* eds. S. A. David, H. Smartt, J. Lippold and J. M. Vitek, ASM International, Ohio, USA (2003) 902–905.

26. A. Ohta, N. Suzuki, Y. Maeda, K. Hiraoka and T. Nakamura: *International Journal of Fatigue* **21** (1999) S113–S118.
27. A. Ohta, N. Suzuki and Y. Maeda: *Properties of Complex Inorganic Solids 2,* ed A. Meike, Kluwer Academic/Plenum Publishers (2000) 401–408.
28. A. Ohta, K. Matsuoka, N. T. Nguyen, Y. Maeda and N. Suzuki: *American Welding Journal* **82** (2003) 77s–83s.
29. J. Eckerlid, T. Nilsson and L. Karlsson: *Science and Technology of Welding and Joining* **8** (2003) in press.
30. Christian, J. W.: *Acta Metallurgica* **6** (1958) 377–379.
31. C. Mack: *Proc. Cambridge Philosophical Society* **52** (1956) 246.
32. H.K.D.H. Bhadeshia and D.V. Edmonds: *Metallurgical Transactions A* **10A** (1979) 895–907.
33. E. Swallow and H. K. D. H. Bhadeshia: *Materials Science and Technology* **12** (1996) 121–125.
34. R. F. Hehemann: *Phase Transformations,* ASM, Metals Park, Ohio, USA (1970) 397–432.
35. H. K. D. H. Bhadeshia: *Bainite in Steels,* 2nd edition, Institute of Materials, London (2001) 1–458.
36. L.–C. Chang and H. K. D. H. Bhadeshia: *Materials Science and Technology* **11** (1995) 874–881.
37. S. B. Singh and H. K. D. H. Bhadeshia: *Materials Science and Engineering A* **A245** (1998) 72–79.
38. F. G. Caballero, H. K. D. H. Bhadeshia, K. J. A. Mawella, D. G. Jones and P. Brown: *Materials Science and Technology* **18** (2002) 279–284.
39. C. Garcia–Mateo, F. G. Caballero and H. K. D. H. Bhadeshia: *Proceedings of ICOMAT '02, Journal de Physique Colloque* (2003) in press.
40. C. G. Mateo, F. G. Caballero and H. K. D. H. Bhadeshia: *ISIJ International* **43** (2003) paper 1, in press.
41. C. G. Mateo, F. G. Caballero and H. K. D. H. Bhadeshia: *ISIJ International* **43** (2003) paper 2, in press.
42. N. Tsuji, R. Ueji, Y. Minamino and Y. Saito: *Scripta Materialia* **46** (2002) 305–310.
43. R. Ueji, N. Tsuji, Y. Minamino and Y. Koizumi: *Acta Materialia* **50** (2002) 4177–4189.
44. H. K. D. H. Bhadeshia: *Materials Science Forum* **284–286** (1998) 64–77.